



HAL
open science

Non thermal plasma in liquid media: Effect on inulin depolymerization and functionalization

Raluca Nastase, Elodie Fourre, Mathieu Fanuel, Xavier Falourd, Isabelle Capron

► **To cite this version:**

Raluca Nastase, Elodie Fourre, Mathieu Fanuel, Xavier Falourd, Isabelle Capron. Non thermal plasma in liquid media: Effect on inulin depolymerization and functionalization. Carbohydrate Polymers, 2020, 231, pp.115704. 10.1016/j.carbpol.2019.115704 . hal-02944380

HAL Id: hal-02944380

<https://hal.inrae.fr/hal-02944380v1>

Submitted on 27 Nov 2020

HAL is a multi-disciplinary open access archive for the deposit and dissemination of scientific research documents, whether they are published or not. The documents may come from teaching and research institutions in France or abroad, or from public or private research centers.

L'archive ouverte pluridisciplinaire **HAL**, est destinée au dépôt et à la diffusion de documents scientifiques de niveau recherche, publiés ou non, émanant des établissements d'enseignement et de recherche français ou étrangers, des laboratoires publics ou privés.



Distributed under a Creative Commons Attribution - NonCommercial - NoDerivatives 4.0 International License

1 **Non thermal plasma in liquid media: effect on inulin depolymerization and** 2 **functionalization**

3 Raluca Nastase^{1,2}, Elodie Fourré¹, Mathieu Fanuel², Xavier Falourd², Isabelle Capron²

4 ¹*Research unit on catalysis and unconventional media, IC2MP, Poitiers, France*

5 ²*UR1268 Research unit Biopolymers, interactions and assemblies (BIA), INRA, Nantes, France*

6 *Corresponding author: elodie.fourre@univ-poitiers.fr*

7 Keywords

8 Gas-liquid plasma reactor; non thermal plasma; inulin; depolymerization; infrared
9 spectroscopy; ssNMR spectroscopy

10 Highlights

- 11 • A novel double dielectric barrier discharge plasma reactor with a liquid interface has
12 been designed
- 13 • It is possible to totally convert inulin into 100 % fructose and glucose
- 14 • No degradation products are generated
- 15 • Combined analytical results evidenced the acidic attack of the glycosidic bond leading
16 to depolymerization

17 Abstract

18 We report the complete conversion of inulin in gas/liquid media by a dielectric barrier discharge
19 plasma at atmospheric pressure. Depending on the plasma treatment time (from 1 to 30 min)
20 and the chemical nature of the gases (air, oxygen, nitrogen), it was possible to depolymerize
21 inulin into fructo-oligosaccharides with a degree of polymerization inferior to 5 or to achieve a
22 total conversion of inulin into its two monomeric constituents, fructose and glucose in 20 min,
23 without any degradation products. Combined results from liquid chromatography (HPLC),
24 solid state Nuclear Magnetic Resonance (ssNMR) and mass spectroscopy revealed that the
25 breakage of the β 1-4-bridged oxygen occurs by an acidic attack, following the oxidation of the

26 polymer. Infrared spectroscopy revealed the oxidation and breakage of the polymer and also
27 adsorption of nitrate species.

28 Introduction

29 Since the industrial revolution, chemistry has developed processes, catalysts and technologies
30 for the conversion of fossil carbon, aiming to create complex and diverse molecules. However,
31 increasing environmental awareness is prompting scientists and manufacturers to develop
32 strategies for environmental sustainability by using processes and materials with low cost, low
33 energy consumption and low toxicity. For several years now, a new approach has been focusing
34 on the use of new raw material from the biomass or waste (Ong et al., 2019; Sheldon, 2018).
35 This change of strategy was revolutionary in the world of chemistry and it has dramatically
36 changed the way a process is designed (Jérôme, Chatel & De Oliveira Vigier, 2016; Farmer &
37 Mascal, 2015; Sylla-Iyarreta Veitía & Ferroud, 2015; Horváth & Anastas, 2007; Baig & Varma,
38 2012; Benoit et al., 2012). For this reason, the use of advanced technologies, such as non-
39 thermal plasma, ultrasounds or ball-milling have been extensively investigated (Farmer &
40 Mascal, 2015). Current and future society needs scientists and manufacturers to focus on new
41 strategies and develop low cost processes for sustainable materials, easy to produce and widely
42 available (Jérôme, 2016)

43 The recent extensive use of non-thermal plasma is the result of a range of reaction parameters
44 that cannot be accessible otherwise, or to a lesser extent. No other media can provide gas
45 temperatures or energy densities as high as those of plasmas; no other media can excite atomic
46 and molecular species to radiate as efficiently; no other media can be arranged to provide
47 comparable transient and non-equilibrium conditions (National Research Council, 1991). This
48 technology is safe, versatile, easy to carry out and allows the generation of highly reactive
49 chemical species with low energy consumption, low toxicity and the possibility of continuous
50 processing (Kan, Lam, Chan, & Ng, 2014).

51 The development of atmospheric pressure plasma technologies has dramatically increased in
52 recent years due to their potential impact in a very wide range of applications that include
53 surface treatments (cleaning, etching), surface activation, surface coating (air plasma spray,
54 plasma enhanced chemical vapor deposition) (Tendero, Tixier, Tristant, Desmaison &
55 Leprince, 2006), but also food (decontamination, toxin degradation, packaging), medicine
56 (sterilization, wound healing, skin treatments) and water (pesticide and dyes degradation,
57 decontamination) (Pankaj & Keener, 2017). The technological progress has encouraged the
58 interest and advancement in the understanding of plasmas. The possibility of performing
59 reactions at atmospheric pressure is becoming increasingly attractive and the fundamental and
60 essential role of technological plasmas is set to expand significantly in the coming years
61 (Mariotti, Patel, Švrček & Maguire, 2012).

62 In this context, production of fructose from fructans such as inulin using plasma, is an
63 alternative to the current approaches, such as acid or enzymatic hydrolysis (Raccuia et al.,
64 2016). Inulin is constituted of fructose units connected by β (1-2) linkages with a glucose at its
65 extremity linked in α (1-2) form. In the inulin chain, the fructose is blocked in the furanose form
66 and glucose is in glucopyranose form. Inulin, its derivatives and its two constitutive monomers
67 have received considerable interest as food ingredients (Blecker, Fougny, Van Herck,
68 Chevalier & Paquot, 2002). Inulin has also been chemically modified in several ways (neutral,
69 anionic, and cationic modification as well as cross-linking and slow release applications) to
70 obtain highly biodegradable compounds at the industrial scale (Stevens, Meriggi & Booten,
71 2001).

72 The effect of non-thermal atmospheric plasma on inulin was already investigated on solid
73 material in gas phase but the reaction mechanism was not completely elucidated [Nastase,
74 Tatibouët & Fourré, 2018; Benoit & al., 2012). The authors reported the depolymerization of
75 inulin with a yield of 16 wt % of fructose (other products being fructo-oligosaccharides (FOS)

76 with a degree of polymerization (DP) lower than 6) via the surrounding water initially contained
77 in polysaccharides that promotes the cleavage of the glycosidic bonds (Benoit & al.). In a recent
78 study (Nastase, Tatibouët & Fourré, 2018), it was suggested that reactive oxidizing species
79 generated by oxygen (ROS) and nitrogen (RNS) played a key role in the depolymerization
80 process, via OH radicals or nitric acid attack.

81 Nowadays, within the field of plasma science and technology, the attention is increasing over
82 the plasma-liquid interactions, and particularly on the physical and chemical mechanisms
83 leading to complex reaction at the plasma-liquid interface (Bruggeman et al, 2016). It is well
84 admitted in the literature that discharges generated at the gas-liquid interface provide gaseous
85 reactive species that can dissolve in the liquid media, inducing the formation of species
86 presenting high reactivity, such as H_2O_2 , $\text{NO}_2^- / \text{NO}_3^-$, OH^\bullet , $\text{HOO}^\bullet / \text{O}_2^{\bullet-}$ to name a few. The
87 fundamental properties of liquid-phase plasma (like generation, state or reactive species) have
88 not been fully described, but the presence of liquid in the system leads to higher reaction rate
89 since the molecular density in the liquid phase is much higher than in the gas phase (Takai,
90 2008). However, plasmas in liquids are more difficult to control and stabilize: the liquid is often
91 an electrode, therefore evaporation and chemical modification occurs, which adds significant
92 complexity compared to the gas phase plasmas (Bruggeman & Leys, 2009).

93 In this respect, a reactor with a double dielectric (DD) barrier, combining a liquid and gas phase
94 DD-LG plasma has been developed. The configuration of the reactor used along this study
95 allows the initiation of various types of reactions: plasma active species formed in the gas and
96 at the gas-liquid interface are further transferred into the liquid giving rise to more chemical
97 reactions. The novelty of this configuration resides in the isolation of the liquid phase between
98 the 2 electrodes, which can avoid problems like electrode evaporation (when using liquid
99 electrode) or contamination from the metal electrode in contact with the liquid. This plasma
100 configuration has been used to follow depolymerization of inulin into FOS, fructose and glucose

101 investigated in controlled conditions in power, time, chemical nature of the gas phase and
102 sample concentration.

103 1. Experimental

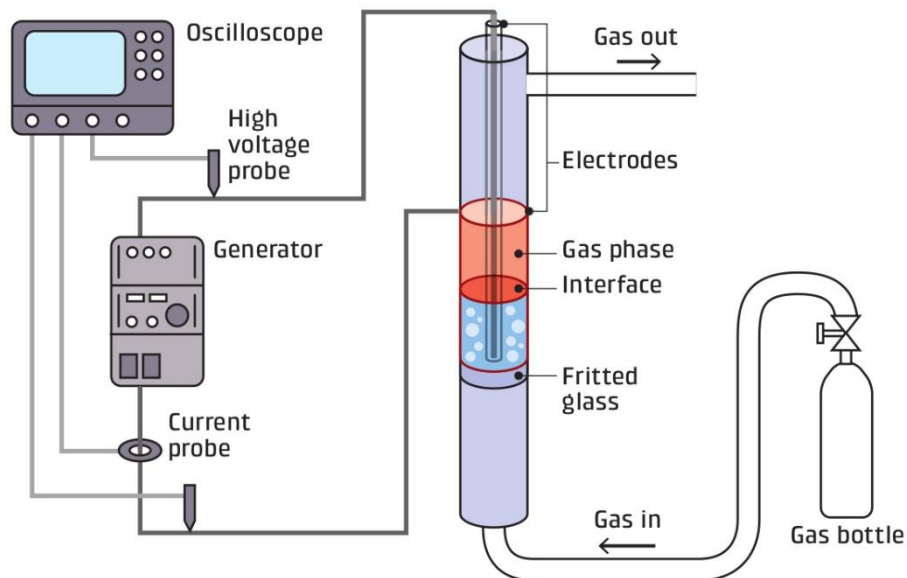
104 1.1. Materials

105
106 Throughout this study, commercial inulin (from chicory, Sigma Aldrich) was used as a
107 substrate. Inulin was solubilized in ultra-pure water under stirring at room temperature, to
108 obtain a concentration of 8 g.L⁻¹ without further treatment.

109 1.2. Gas-liquid plasma device

110
111
112 Plasma treatment was carried out in a dielectric barrier discharge reactor consisting in a double
113 wall glass cylinder separated in two parts by a fritted glass (figure 1). This reactor can be
114 classified as multiphase discharge (Bruggeman et al., 2016) except that both electrodes are
115 isolated from the liquid phase by two glass walls. The first electrode (inox tube) stands in the
116 center of the cylinder and was protected from the liquid by a first dielectric wall. The second
117 electrode (copper adhesive tape, from Advance tape) was wrapped around the second dielectric
118 wall, on the outside wall of the cylinder. The gap between both dielectrics was 3 mm. A high
119 voltage supply (A2E Technologies Enertronic), was connected to the electrodes and providing
120 bipolar voltage pulses, allows the variation of the voltage from 0 to 40 kV. The gas (flow of 30
121 mL.min⁻¹) was introduced in the reactor from the bottom entry and was flown through a fritted
122 glass which not only created bubbles, but also prevented the liquid from draining. The volume
123 of the solution to be treated was set at 5 mL, allowing the generation of plasma in the gas phase,
124 right above the surface of the liquid and, in a lesser extent, in the gas bubbles through the liquid.
125 The solution was injected in the system kept at atmospheric pressure, room temperature and
126 with the gas flow set at 30 mL min⁻¹. In order to determine the optimal parameters for inulin
127 conversion, the electrical parameters (voltage, 16-21 kV) and the treatment time (1-40 min)

128 were modified. The discharge was generated under nitrogen, oxygen, helium and air
129 atmosphere



130

131 Figure 1: Drawing of the experimental setup

132

133 1.3.Characterization

134 *Hydrogen peroxide content*

135

136 Hydrogen peroxide produced during the plasma treatment was calculated from colorimetric
137 titration with potassium permanganate, in acidic conditions. 10 mL of plasma treated sample
138 was placed in a beaker with 20 mL distilled water and 10 mL of H₂SO₄ solution (3 M). The
139 solution was magnetically stirred and a solution of KMnO₄ (0.025 M) was added dropwise
140 through a graduated burette. The concentration was calculated from the equivalent point
141 volume.

142 *HPLC*

143 High Pressure Liquid Chromatography was used to determine the presence of oligosaccharides
144 after plasma processing. Samples were analyzed on a Shodex Sugar KS-802 column
145 (maintained at 40°C) that allows the separation of oligosaccharides by steric exclusion and

146 ligand exchange. The stationary phase consists of polystyrene-divinylbenzene coated with a
147 cation exchange resin and the mobile phase consists of ultra-pure water at a flow rate of 1
148 mL.min⁻¹.

149 Molecules were eluted depending on their hydrodynamic volume. The concentrations of
150 fructose and glucose were defined for each compound by a calibration curve established with
151 different concentrations (supplementary information), giving the concentration in g.L⁻¹ of the
152 analyzed compound as a function of the area of the chromatographic peaks.

153 *Solid state Nuclear Magnetic Resonance*

154 Solid state ¹³C NMR experiments were carried out using a Bruker Avance III 400 MHz
155 spectrometer operating at a ¹³C frequency of 100.62MHz and equipped with a CP/MAS 4 mm
156 ¹H/¹³C probe. Prior to the analysis, the samples were neutralized with a solution of NaOH (0.1
157 M) and lyophilized. The pH was measured with a pHmeter (Eutech instrument pH510). The
158 solid samples were packed in a 4 mm NMR rotor without any other preparation. The sample
159 were spun at a rate of 9 kHz at room temperature. The cross polarization pulse sequence
160 parameters were as follow : 3.95 μs for proton 90° pulse, a contact time between 0.8 and 2.0
161 ms and 10 s recycle time. Usually, the accumulation of 5120 scans was used. The carbonyl
162 signal of glycine (176.03 ppm) was used to calibrate the chemical shift of the ¹³C NMR spectra.
163 The chemical shift, peak half-width and peak area of the different peaks were determined with
164 a least squares fitting method using Peakfit® software

165 *Mass spectrometry*

166
167 The samples analyzed by ssNMR were also analyzed by matrix-assisted laser
168 desorption/ionization (MALDI)-time-of-flight (TOF) MS. For the measurements, an ionic
169 preparation of 2,5-dihydroxybenzoic acid (DHB) and N,N-dimethylaniline (DMA) was used as
170 the MALDI matrix, as described in (Ropartz, 2011). Briefly, the matrix consists of a mixture

171 of DHB and DMA (DHB 100 mg.ml⁻¹, in H₂O/acetonitrile/ DMA (1:1:0.02)) and was mixed
172 with the samples in a 1:1 ratio (v/v). The mixture (1 μL) was then deposited on a polished steel
173 MALDI target plate. MALDI measurements were then performed on an Autoflex Speed
174 MALDI-TOF/TOF spectrometer (Bruker Daltonics, Bremen, Germany) equipped with a
175 Smartbeam laser (355 nm, 1000 Hz) and controlled using the Flex Control 3.0 software
176 package. The mass spectrometer was operated with positive polarity in reflectron mode. Spectra
177 were acquired in the range of 180–3500 *m/z*.

178 The evolution of the percentage of DP 1 was then monitored using the following formula:

179
$$\% = \frac{I_{DP1}}{I_{DP1}+I_{DP2}+I_{DP3}+I_{DP4}} \quad \text{equation 1}$$

180 *FT-IR*

181 Fourier transform infrared spectroscopy was performed before and after plasma treatment in
182 order to observe the eventual functionalization and/or stabilization of species on the surface of
183 inulin. Prior to analysis, the sample was lyophilized. The powder sample (5 mg) was mixed
184 with KBr (100 mg) and pressed in a hydraulic press and then recovered in the form of a pellet.
185 The analysis was carried out in a Nicolet IS50 spectrometer in transmission mode and the
186 resulting spectra were an average of 200 scans at a resolution of 16 cm⁻¹. All spectra were
187 baseline corrected and normalized to be compared to each other.

188 2. Results and discussion

189 2.1. Reactor optimization

190

191 In order to identify the reactivity sites (in gas bubbles, in the upper gas phase or at liquid-gas
192 interface) and to evaluate the discharge propagation, the effect of the volume of liquid submitted
193 to plasma was studied, introducing 5 mL, 10 mL and 15 mL of an aqueous solution of inulin at
194 8 g.L⁻¹ (figure 2). The experiments were carried out at constant voltage (19 kV), frequency (2
195 kHz) and time (20 min). The efficiency of the plasma discharge was evaluated by its impact on

196 inulin depolymerization via the following of fructose yields, pH, and $\text{NO}_2^- / \text{NO}_3^-$ and H_2O_2
197 concentrations.

198 When 15 mL were introduced, the inulin solution filled the reactor with 5 mL of the volume
199 standing above the external electrode limit. No depolymerization occurred in this configuration.
200 Additionally, no pH change was observed and no other species were detected (Table 1). It
201 appeared that the observed discharge was occurring in the tube holding the central electrode, as
202 a very small air gap was present between the electrode and the inner wall of the dielectric barrier
203 (visible on figure 1). When the inner tube was sealed with glue, no plasma discharge was
204 observed, neither depolymerization.

205 When 10 mL of solution were inserted in the reactor, it allowed the development of the plasma
206 at the gas-liquid interface but without (or very little) plasma in the gas phase. A concentration
207 of only 0.14 g.L^{-1} of fructose was detected and, in the same time, pH dropped from 6.5
208 (untreated solution) to 5.0. Using semi quantitative test strips (Quantofix), a small fraction of
209 NO_x^- species were measured indicating the dissolution of nitrous oxides into nitrites (1 mg.mL^{-1})
210 and nitrates ($\leq 10 \text{ mg.mL}^{-1}$).

211 Finally, 5 mL of solution introduced resulted in a system with two phases of plasma, at interface
212 and in the gas phase. In this case, inulin was totally depolymerized into fructose (7 g.L^{-1}),
213 glucose (0.25 g.L^{-1}) and a compound of DP 2. It clearly showed that the most effective reaction
214 occurred when the gas-liquid interface and even more importantly, the plasma in gas phase are
215 present. From these results, the configuration using 5 mL of solution was kept throughout the
216 study.

217 The fact that the depolymerization was enhanced in presence of a gas phase highlighted the fact
218 that the long lived plasma species from the gas phase may be responsible of the reactivity. Their
219 dissolution in the liquid media would lead to active species capable to dissociate the polymer.

220 In order to verify this hypothesis the reactor was turned upside down, allowing only the contact
 221 of the plasma long lived species with the liquid. It resulted in no modification of the inulin
 222 chain. The pH of the solution decreased to 3.4, indicating the dissolution of acidic species from
 223 the gas phase in the liquid, but no depolymerization occurred. It has been established in the
 224 literature (Bruggeman et al., 2016; Takai, 2008) that the active species generated in the gas
 225 phase are transferred from the gas to the liquid phase, creating more reactive species such as
 226 H₂O₂, peroxonitrites (ONOO⁻) and nitric acid (HNO₃). Among the species commonly produced
 227 in the liquid phase, H₂O₂, NO₂⁻ and NO₃⁻ were detected in the samples after plasma treatment
 228 (Table 1). In the case of air treatment, NO₃⁻ was detected up to 500 mg.mL⁻¹.

229 Table 1: pH, NO₂⁻ / NO₃⁻ and H₂O₂ concentrations measured after 20 min of air plasma treatment
 230 for different liquid volumes. Parameters: P = 28 W, gas flow = 30 mL.min⁻¹, f = 2 kHz; [inulin]
 231 = 8 g.L⁻¹

| Volume | 15 ml | 10 ml | 5 ml | Upside down (5 mL) |
|---|-------|-------|------|--------------------|
| pH | 6.5 | 5 | 1.5 | 3.4 |
| H ₂ O ₂ mg.mL ⁻¹ | 0 | 10 | 11.2 | 1.5 |
| NO ₂ ⁻ mg.mL ⁻¹ | 0 | 1 | 15 | 0 |
| NO ₃ ⁻ mg.mL ⁻¹ | 0 | 15 | 500 | 350 |

232

233 2.2. Varying the chemical nature of the plasma gas

234

235 In order to further identify and evaluate the reactivity of plasma chemical active species in such
 236 a system, the depolymerization reaction of inulin was performed using different gases. The
 237 results are summarized in table 2. The highest concentration of H₂O₂ was measured under
 238 oxygen and O₂/He plasma. Under nitrogen and air plasma the H₂O₂ concentrations were lower,
 239 due to the presence of NO₂⁻, which in acidic conditions can lead to the H₂O₂ degradation

240 (Gorbanev, O'Connell & Chechik, 2016; Lukes, Dolezalova, Sisrova & Clupek, 2014). The
 241 lowest concentration was measured under pure helium plasma.

242 Table 2: fructose concentration, pH and oxidized species concentrations measured after 20 min
 243 of plasma treatment for different gas phases. Parameters: gas flow = 30mL.min⁻¹, f = 2 kHz;
 244 [inulin] = 8 g.L⁻¹

| Gas nature | 100 % O ₂ | 100 % He | 50% He / 50% O ₂ | 100 % N ₂ | Synthetic air |
|---|----------------------|----------|-----------------------------|----------------------|---------------|
| Power (W) | 12 | 12 | 28 | 14 | 28 |
| Fructose conc. (g.L ⁻¹) | 0.3 | 0.02 | 0.3 | 0.9 | 7 |
| pH | 3-4 | 3-4 | 3-4 | 1.5 | 1.5 |
| H ₂ O ₂ (mmol.L ⁻¹) | 15.5 | 3.6 | 13.7 | 10 | 11.2 |
| NO ₃ ⁻ (mg.L ⁻¹) | none | none | none | 250 ≥ x ≥ 500 | ≥ 500 |
| NO ₂ ⁻ (mg.L ⁻¹) | none | none | none | 5 < x < 10 | 15 |

245
 246 The fructose concentration measured after plasma treatment under helium was the lowest (0.02
 247 g.L⁻¹). The actives species generated under helium plasma such as He^{*}, He₂^{*}, He⁺ and He₂⁺, but
 248 also dissolved oxygenated species generated from electron and helium impact on water
 249 molecules, are not participating in the reaction in the first 30 min. Oxygen gas appeared also
 250 quite inert since the addition of oxygen to helium gas and higher injected power in the reactor
 251 did not affect the fructose yield as compared with pure oxygen (0.3 g.L⁻¹). When pure nitrogen
 252 was flown through the system, a slight increase of fructose concentration was observed but to
 253 a lesser extent compared to air treatment where inulin was totally converted. It is worth
 254 mentioning that an air plasma treatment at 12W resulted in no conversion.

255 The HPLC results of the plasma treatment under synthetic air showed the progressive
 256 depolymerization of inulin into smaller fractions and its two constituents, glucose and fructose.
 257 Air plasma is the most effective treatment for the inulin depolymerization. A treatment time of
 258 approximately 20 min allowed the total conversion of inulin (figure 2). The concentration of
 259 fructose was 7 g.L⁻¹ reaching a plateau at 20 and 30 min. Interestingly, the glucose concentration

260 (figure 2b) increased until 30 min of treatment (0.4 g.L^{-1}). It appears that the reactive species
261 derived from the reactions between nitrogen and oxygen in the air plasma are responsible for
262 the depolymerization. Nitrous oxides solvation in water would lead to nitric and nitrous acids,
263 providing H^+ ions and consequently acid hydrolysis of the polymer.

264

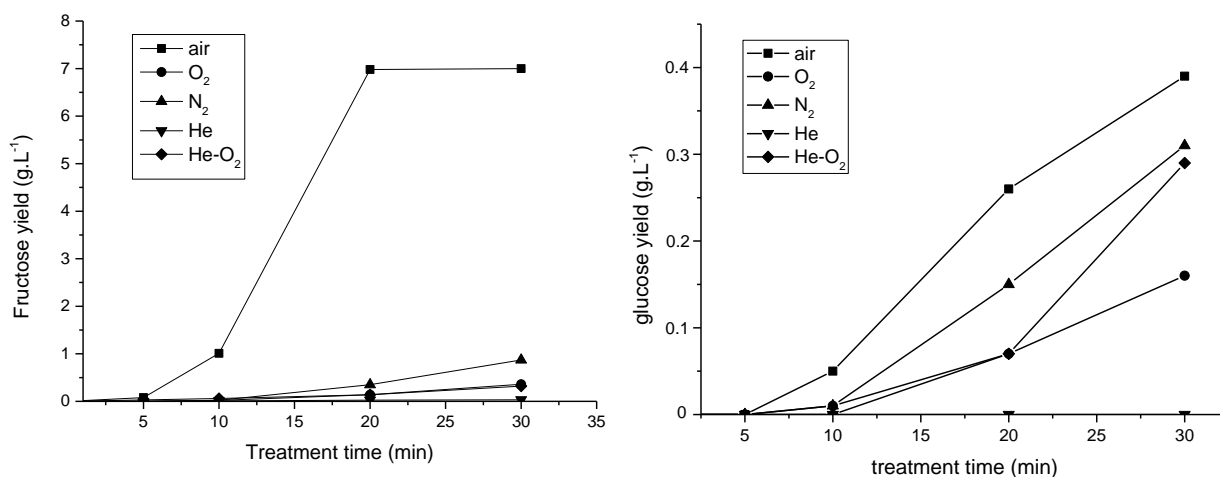
265

266

267

268

269



270 Figure 2: plot of a) fructose and b) glucose yields as a function of treatment time. Conditions: 2 kHz, 30
271 mL.min⁻¹; P = 28 W and P (He) = 12 W; [inulin] = 8 g.L⁻¹

272

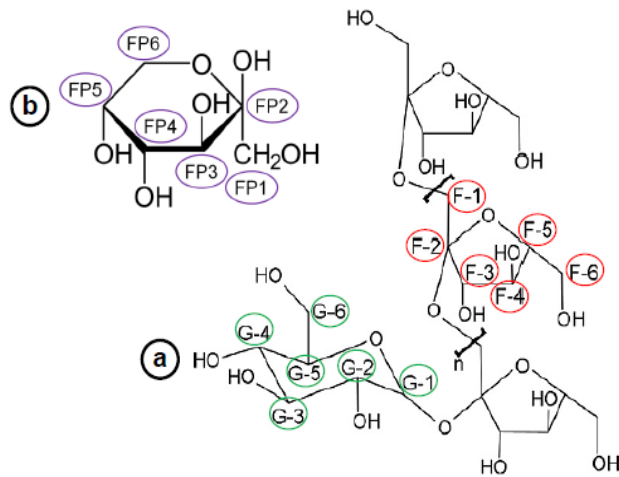
273 A series of tests with nitric acid were performed in order to confirm this hypothesis. When 5ml
274 of inulin solution were mixed with nitric acid (1 mol.L^{-1}) till a pH = 1.5, followed by 80°C
275 heating from 20 to 100 min, a total conversion into fructose (8 mg.ml^{-1}) was achieved. The same
276 result was obtained when inulin powder was added to plasma treated water (in air; P = 28 W)
277 and heated up at 80°C. The pH of the water treated with air plasma equaled 1.5. These
278 experiments confirmed the participation of H^+ in the depolymerization process.

279 2.3.Elucidating the depolymerization process

280

281 ¹³C CP/MAS NMR spectroscopy was used for anomer analyses of reducing terminal units of
282 the treated chains in order to follow depolymerization under air plasma treatment, which proved
283 to be the most efficient treatment. A freeze dried reference (no plasma) was prepared and
284 compared to samples treated in air up to 20 min. The structure of inulin (a), along with the β -

285 D-fructopyranose form (b) detected in some samples is represented in figure 6. When
 286 glucopyranose is present at the reducing end, the fructose molecules are in the furanose form.
 287 Without glucose at the end, the fructose molecules are in the pyranose form (Levy & Fügedi,
 288 2005). The labelling on the NMR spectra are also referenced in figure 3.



289
 290 Figure 3: Structure of a) inulin and b) β -D-fructopyranose

291
 292 After spectral deconvolution, the average degrees of polymerization have been calculated using
 293 the next formula:

294 For untreated inulin, the lyophilized untreated inulin and inulin treated by plasma for 3 min:

$$295 \quad DP \text{ average} = \frac{\left[\frac{\sum \text{area from 83 to 57 ppm}}{5} \right] - \text{area at 93 ppm}}{\text{area at 93 ppm}} \quad \text{Equation 2}$$

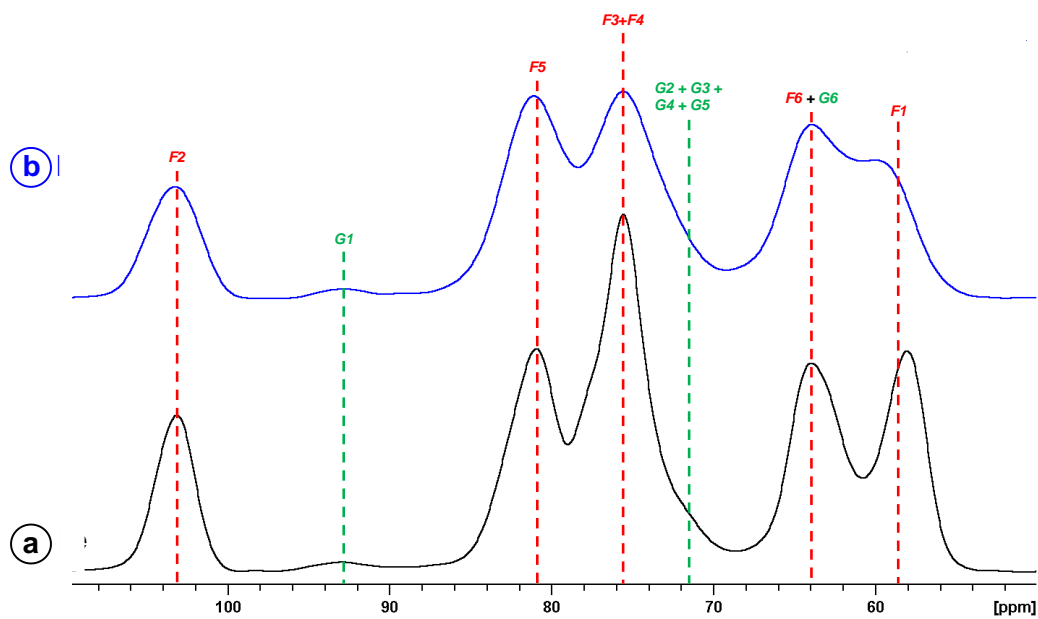
296 The numerator corresponds to the signal of fructose monomers subtracted from glucose
 297 contribution (figure 4). The denominator corresponds to the signal of anomeric carbons of
 298 ending glucose.

299 Inulin treated by plasma from 7 to 40 min:

$$300 \quad DP \text{ average} = \frac{[(\sum \text{area from 83 to 57 ppm})/5] - (\text{area at 93 ppm} + \text{area at 98 ppm})}{(\text{area at 93 ppm} + \text{area at 98 ppm})} \quad \text{Equation 3}$$

301 The peak at 93 ppm corresponds to the glucose reducing end in the α conformation and the
302 peak at 98 ppm in the β conformation or C₂ from fructopyranose (Colombo, Aupic, Lewis &
303 Mario Pinto, 2015).

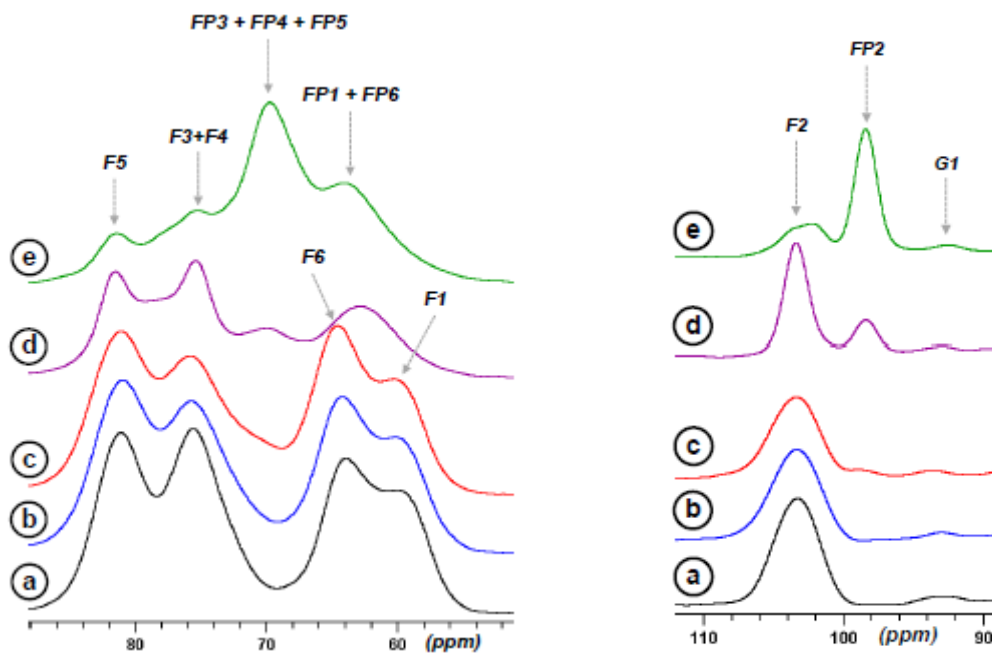
304 The NMR analysis of the freeze dried reference (figure 4) highlighted the presence of
305 fructopyranose form of inulin and showed that the freeze-drying step was also affecting the
306 supramolecular organization of inulin. The widening of the bands at 103 ppm and in both
307 regions 86-70 ppm and 68-54 ppm reflected a less ordered structure after lyophilization, most
308 probably arising from a loss of the crystallinity. In addition, the chemical shift of C₁ (F1) of
309 fructose, between 80 and 74 ppm, was modified suggesting a significant change of the magnetic
310 environment.



311

312 Figure 4: ¹³C CP/MAS inulin spectra, (a) initial state, (b) after solubilization and lyophilization.
313 (Annotations are referring to figure 3).

314



315

316 Figure 5: ^{13}C CP/MAS spectra zones of non-anomeric carbons (left panel) and anomeric carbon (right
 317 panel) of (a) lyophilized inulin (reference) and after plasma treatment of (b) 3 min, (c) 7 min,
 318 (e) 20 min. (Annotations are referring to figure 6)

319

320 Figure 5 shows the ^{13}C CP/MAS spectra of inulin before and after up to 20 min of plasma
 321 treatment. As the time of plasma treatment increased, peaks in the 110 – 90 ppm and 90 – 55
 322 ppm regions evolved differently. The anomeric and non-anomeric carbon peaks of furanose
 323 ring, labelled F1 to F6, are decreasing as the treatment time increases. At 7 min of treatment,
 324 an anomeric carbon (FP2) presenting a chemical shift at 98.4 ppm is emerging, identified as C₂
 325 carbons of free fructose in the β -D-fructopyranose form (Colombo, Aupic, Lewis & Mario
 326 Pinto, 2015; Shiomi & Onodera, 1990). The proportion of this signal increases with treatment
 327 time. The presence of free β -D-fructopyranose is confirmed by peaks in the non-anomeric
 328 carbon region at 70 ppm and 84 ppm, which increases as a function of treatment time. It is
 329 worth mentioning that the pyranose form of fructose was predominant during the solubilization
 330 step of monomeric fructose. This result indicates that the conversion from the furanose to

331 pyranose form is most likely to occur during the neutralization step and is not due to the plasma
332 treatment.

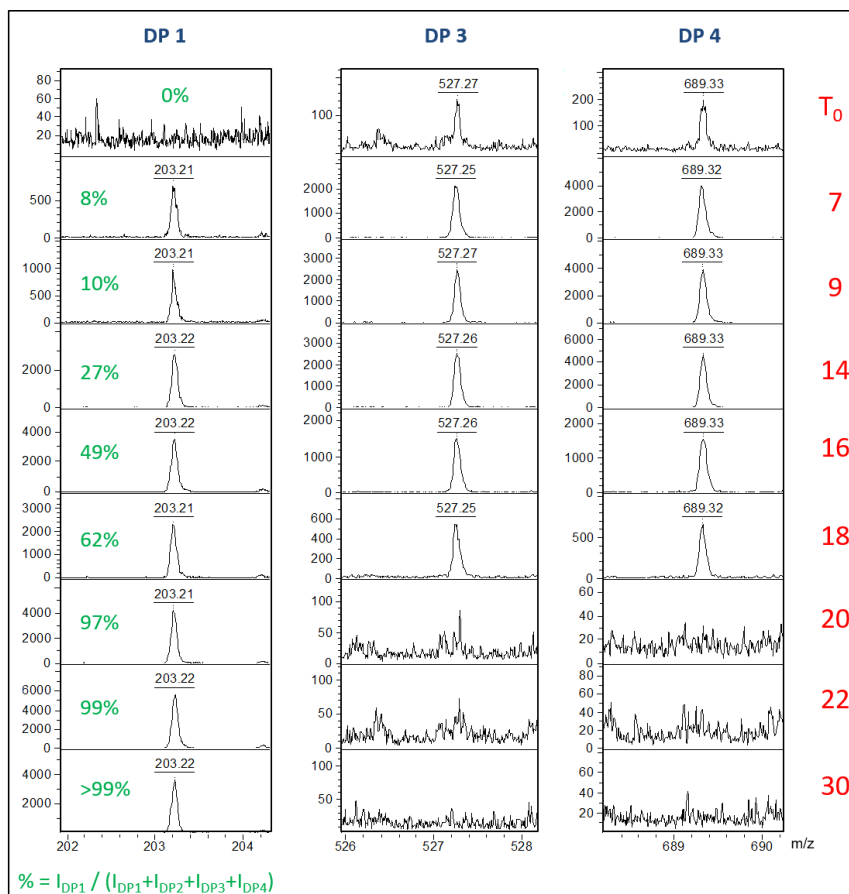
333 From equations (2) and (3), average values of the degrees of polymerization were calculated
334 (table 3). It shows that after 3 min, a clear depolymerization occurs as already shown by the
335 HPLC. A progressive decrease of the DP was observed as a function of the plasma treatment
336 time up to monomers, without further degradation.

337 Table 3: Calculated average degree of polymerization (DP) of air plasma treated inulin: P = 28 W; f = 2
338 kHz; flow rate: 30 mL.min⁻¹

| | DP |
|--------------------|----|
| Commercial inulin | 30 |
| Lyophilized inulin | 29 |
| 3min | 27 |
| 7min | 13 |
| 13min | 3 |
| 20min | 1 |

339

340 To investigate the molecular polydispersity of the released products and more specifically the
341 proportion of DP 1 throughout the treatment of inulin by the plasma, MALDI-TOF MS analyses
342 were performed (figure 6). The evolution of the proportion of DP 1 compared to DP 2, 3 and 4
343 was monitored by mass spectrometry, using the equation 1. These experiments showed that
344 above 20 min, it remains almost only DP 1 species (glucose and/or fructose). This result is
345 according to NMR measurements.



346

347 Figure 6: Evolution of the signal of DP 1, 3 and 4 by mass spectrometry as a function of plasma treatment
 348 time. Oligosaccharides are detected as sodium adducts. The percentage of DP 1 was determined using
 349 equation 1. The DP2 is not represented for esthetic reason, due to the presence of numerous matrix peaks
 350 in the same region.

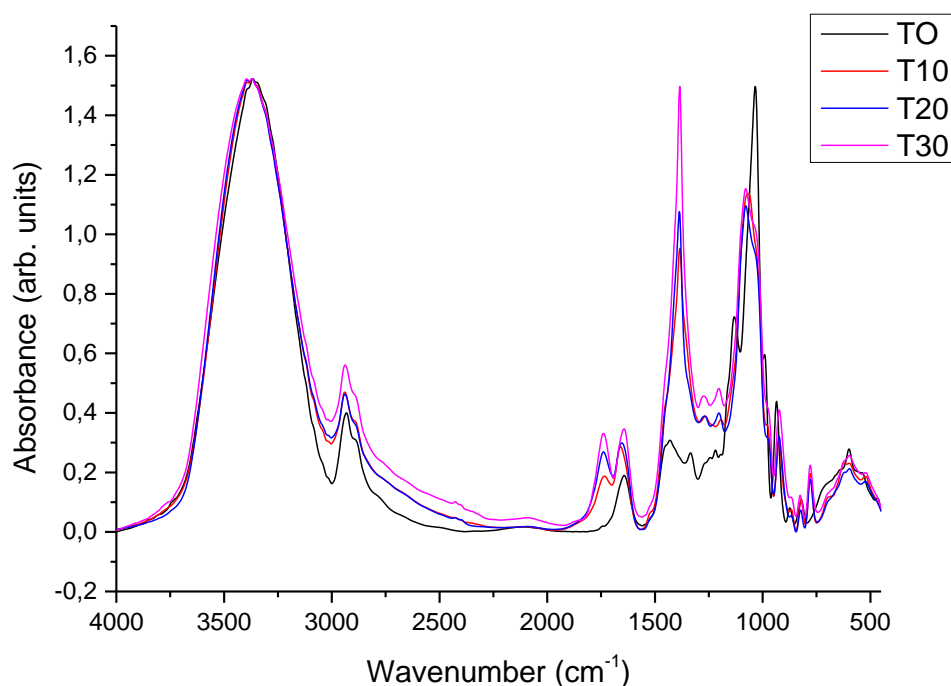
351

352 While fructose and glucose both crystallize as cyclic forms, in solution the free sugars show an
 353 equilibrium with an acyclic form in small amount, the formation of which creates a carbonyl
 354 group (Levy & Fügedi, 2005). This carbonyl group can react with hydroxyl groups restructuring
 355 the hemiacetal cyclic form. For six carbon carbohydrates, like glucose and fructose, the ring
 356 closing reaction can occur with more than one hydroxyl group, leading to isomerization and
 357 multiple cyclic forms. Inulin is relatively chemically inert, although cleavage of the polymer
 358 chain at any of the glycosidic bonds will produce a reactive reducing end, prone to further
 359 reaction (Stevens, Meriggi & Booten, 2001; Wack & Blaschek, 2006).

360 2.4. Infrared bands attribution

361

362 Infrared analysis was used routinely for the assessment of chemical structure of treated inulin.
363 The full IR description of raw inulin has been described elsewhere (Grube, Bekers, Upite &
364 Kaminska, 2002; Ibrahim, Alaam, El-Haes, Jalbout & de Leon, 2006; Wack & Blaschek, 2006),
365 and can be used as reference. In the first region, between 4000-2000 cm^{-1} , the large broad band
366 at 3300 cm^{-1} , corresponding to the stretching of OH groups, did not change during the plasma
367 treatment (Figure 7). A sharp band of middle intensity was noticeable at 2930 cm^{-1} , assigned to
368 the valence vibration of C-H asymmetric stretching of CH_2 and a shoulder at 2890 cm^{-1}
369 attributed to C-H symmetric stretching of CH_2 . A deviation of the baseline with treatment time,
370 giving rise to a broad absorption between 2400 - 3000 cm^{-1} was attributed to the formation of
371 carboxylic acids, under their dimeric form (Bellamy, 1962).



372

373 Figure 7: Infrared spectra of inulin as a function of plasma treatment time

374 In the following region, between 2000 and 1100 cm^{-1} , multiple modifications were observed.
375 Plasma treated samples showed the formation of a new band at 1740 cm^{-1} , corresponding to
376 stretching vibrations of C=O group. The band at 1640 cm^{-1} , based on the existing literature

377 (Higgins, Stewart & Harrington, 1961), was assigned to adsorbed water. The light shift of the
378 band to 1660 cm^{-1} was attributed to a change of the electronic environment due to intermediate
379 states generated during the oxidation steps, i.e. C=O formation. The bands at 1430 and 1334
380 cm^{-1} of the raw inulin are no longer visible after plasma treatment, hidden by the intensive broad
381 band at 1385 cm^{-1} , corresponding to adsorbed nitrate ion (Elmelouky, Mortadi, Chahid &
382 Elmoznine, 2018). From T10 to T30, the presence of two bands at 1280 cm^{-1} and at 1205 cm^{-1}
383 indicate a structure modification from the polymer to the monomer as these bands are related
384 to OCH and CCH bending vibrations bands of fructose and glucose. A complete disappearance
385 of the 1130 cm^{-1} band indicates the loss of C-O-C bridge character.

386 In the third region $1100\text{-}500\text{ cm}^{-1}$, also known as the fingerprint region, modifications are also
387 visible. Firstly, the band at 1030 cm^{-1} is reduced and hidden by a band at 1080 cm^{-1} (D-fructose).
388 All the bands ($1035, 990, 935, 872$ and 820 cm^{-1}) related to the fructose/glucose ring structure
389 (C-O-C ring group and ring vibrations) shift slightly towards lower values but are still present,
390 indicating that the integrality of the monomer ring was not affected during the
391 depolymerization. Finally, a new band is formed at 778 cm^{-1} corresponding to CCO and CCH
392 bending of D-fructose and D-glucose. From these data, inulin is depolymerized without
393 degradation of the fructose and glucose rings. First, an oxidation of C-OH groups into
394 carboxylic acids takes place. As the plasma treatment time increases, breakage of the C-O-C
395 bridge of the polymer is observed.

396 It has been established in the literature (Bruggeman & Leys, 2009; Gorbanev, O'Connell &
397 Chechik, 2016; Nastase, Tatibouët & Fourré, 2018; Shainsky, 2012), that various types of
398 plasma-chemical species and reactions are initiated in air plasma in and in contact with liquids.
399 Among the chemical species produced by plasma at the gas-liquid interface, OH^\bullet radical,
400 atomic oxygen, ozone and hydrogen peroxide are the main reactive oxygen species generally
401 accepted (Lukes, Dolezalova, Sisrova & Clupek, 2014; Sunka, 1999) to play the dominant role

402 in the reactivity. As for the nitrogen based species, nitric oxide and its derivatives formed with
403 water (nitrites, nitrates and peroxyxynitrites) are to be considered. For example, the dissolution of
404 the nitrous oxide gas generated in air plasma (Machala, 2013) leads to the formation of nitric
405 and nitrous acids. The most likely reaction pathway for the depolymerization would be via the
406 hydrolysis of the C-O-C bridge from H^+ ions of HNO_3 arising from the NO_x dissolution in the
407 liquid. The slight depolymerization observed in nitrogen free plasmas could be attributed to OH
408 radicals attack of the glycosidic bond. However, this does not explain the decrease of pH after
409 a plasma treatment without nitrogen. Hydrogen peroxide concentration is too low to induce
410 such pH decrease. Literature reports the formation of acids (Machala, 2013; Shainsky, 2012),
411 arising from superoxide ion, O_2^- , that participate in the decrease of pH under nitrogen free
412 plasma discharge and could explain our observation.

413 Conclusions

414 The use of renewable polysaccharide feedstocks to produce chemicals is stimulating a revival
415 in carbohydrate chemistry employing green and sustainable processes. In this study, a new
416 reactor has been successfully designed for the treatment of solutions or suspensions in a double
417 dielectric barrier discharge plasma reactor. This specific reactor configuration was used in the
418 depolymerization reaction of inulin. The conversion was strongly dependent on the gas
419 chemical nature and reactor configuration. Pure gases of helium, nitrogen and oxygen had little
420 effect on the depolymerization. However, plasma treatment under air led to a complete
421 depolymerization into fructose, glucose and a DP2 compound. It appears that reactivity is at
422 play at the gas-liquid interface, where electrons and gas species can be solvated and either attack
423 glycosidic bonds of inulin or recombine into more reactive species. Hydrogen peroxide, nitrous
424 and nitric oxides were identified. It appeared that the breakage of the glycosidic bond is
425 achieved by nitric acid hydrolysis under an air plasma discharge, while OH radicals attack
426 seems to be responsible of the small depolymerization under nitrogen free plasma. There is no

427 doubt with these results that the modification of biomass by non-thermal plasma in liquid media
428 represents a new and non-toxic approach that would reconsider the traditional ways.

429 Acknowledgements

430 The authors would like to thank the financial supports which are ADEME, Pays de Loire Region
431 and the FR CNRS INCREASE 3707 consortium. The mass spectrometry and NMR analyses
432 were performed using the equipment of the BIBS facility in Nantes (UR1268 BIA, IBiSA,
433 Phenome-Emphasis-FR (grant number ANR-11-INBS-0012)).

434 References

- 435
- 436 Baig, RB., & Varma, RS. (2012) Alternative energy input: mechanochemical, microwave and
437 ultrasound-assisted organic synthesis, *Chemical Society Review*, *41*,1559-84
- 438 Bellamy, LJ. (1962) *The infra-red spectra of complex molecules*, Ed. Methuen & Co LTD.
- 439 Benoit, M., Rodrigues, A., De Oliveira Vigier, K., Fourré, E., Barrault, J., Tatibouët J.-M., &
440 Jérôme, F. (2012) Combination of ball-milling and non-thermal atmospheric plasma as physical
441 treatments for the saccharification of microcrystalline cellulose, *Green Chemistry*, *14*, 2212-
442 2215
- 443 Benoit, M., Rodrigues, A., Zhang, Q., Fourré, E., De Oliveira Vigier, K., Tatibouët, J.-M., &
444 Jérôme, F. (2011) Depolymerization of cellulose assisted by a non-thermal atmospheric plasma,
445 *Angewandte Chemie International Edition*, *50*, 8964 –8967
- 446 Blecker, C., Fougnyes, C., Van Herck, J-C., Chevalier J-P., & Paquot, M. (2002) Kinetic study
447 of the acid hydrolysis of various oligofructose samples, *Journal of Agricultural Food*
448 *Chemistry*, *50*, 1602-1607
- 449 Bruggeman, PJ., Kushner, MJ., Locke, BR., Gardeniers, JGE., Graham, WG., Graves, DB.,
450 Hofman-Caris, RCHM., Maric, D., Reid, JP., Ceriani, E., Fernandez Rivas, D., Foster, JE.,

451 Garrick, SC., Gorbanev, Y., Hamaguchi, S., Iza, F., Jablonowski, H., Klimova, E., Kolb, J.,
452 Krcma, F., Lukes, P., Machala, Z., Marinov, I., Mariotti, D., Mededovic Thagard, S., Minakata,
453 D., Neyts, EC., Pawlat, J., Lj Petrovic, Z., Pflieger, R., Reuter, S., Schram, DC., Schröter, S.,
454 Shiraiwa, M., Tarabová, B., Tsai, PA., Verlet, JRR., von Woedtke, T., Wilson, KR., Yasui, K.,
455 & Zvereva, G. (2016) Plasma–liquid interactions: a review and roadmap, *Plasma Sources*
456 *Science and Technologies*, 25, 053002

457 Bruggeman, P., & Leys, C. (2009) Non-thermal plasmas in and in contact with liquids, *Journal*
458 *of Physics D: Applied. Physics*, 42, 053001

459 Colombo, C., Aupic, C., Lewis, A.R., & Mario Pinto, B. (2015) In situ determination of fructose
460 isomer concentrations in wine using ¹³C quantitative nuclear magnetic resonance spectroscopy,
461 *Journal of Agriculture and food chemistry*, 63, 8551 - 8559

462 Elmelouky, A. Mortadi, A., Chahid, El., Elmoznine, R. (2018) Impedance spectroscopy as a
463 tool to monitor the adsorption and removal of nitrate ions from aqueous solution using zinc
464 aluminum chloride anionic clay, *Heliyon*, 4, e00536

465 Farmer, JT., & Mascal, M. (2015). Platform molecules. In Clark, J., Deswarte, & F.,
466 *Introduction to chemicals from biomass*, 2nd Edition (pp.89-156). John Wiley & Sons, Ltd.

467 Gorbanev, Y., O'Connell, D., & Chechik, V. (2016) Non thermal plasma in contact with water:
468 the origin of species, *Chemistry: a European Journal*, 22, 3496-3505

469 Grube, M., Bekers, M., Upite, D., & Kaminska, E. (2002) E. Infrared spectra of some fructans,
470 *Spectroscopy*, 16, 289-296

471 Higgins, HG., Stewart, CM., & Harrington, KJ. (1961) Infrared spectra of cellulose and related
472 polysaccharides, *Journal of polymer chemistry*, 51,59-84

473 Horváth, HT., & Anastas, PT. (2007) Innovations and green chemistry, *Chemical Reviews*, 107,
474 2169-2173

475 Ibrahim, M., Alaam, M., El-Haes, H., Jalbout, AF., & de Leon, (2006) F. Analysis of the
476 structure and vibrational spectra of glucose and fructose, *Ecletica Quimica*, 31, 15-21

477 Jérôme, F. (2016) Non-thermal atmospheric plasma: opportunities for the synthesis of valuable
478 oligosaccharides from biomass, *Current Opinion in Green and Sustainable Chemistry*, 2, 10-
479 14

480 Jérôme, F., Chatel G., & De Oliveira Vigier, K. (2016) Depolymerization of cellulose to
481 processable glucans by non-thermal technologies, *Green Chemistry*, 18, 3903-3913

482 Kan, CW., Lam, CF., Chan, CK., & Ng, SP. (2014) Using atmospheric pressure plasma
483 treatment for treating grey cotton fabric, *Carbohydrate Polymers*, 15, 167-73

484 Levy DE., & Fügedi, P. (2005) *The Organic Chemistry of Sugars*, CRC Press and Taylor and
485 Francis Group

486 Lukes, P., Dolezalova, E., Sisrova, I., & Clupek, M. (2014) Aqueous-phase chemistry and
487 bactericidal effects from an air discharge plasma in contact with water, *Plasma Sources Science
488 and Technologies.*, 23, 015019

489 Machala, Z., Tarabova, B., Hensel, K., Spetlikova, E., Sikurova, L., & Lukes, P. (2013)
490 Formation of ROS and RNS in water electro-sprayed through transient spark discharge in air
491 and their bactericidal effects, *Plasma Process and Polymers*, 10, 649-659

492 Mariotti, D., Patel, P., Švrček, V., & Maguire, P. (2012) Plasma-liquid interactions at
493 atmospheric pressure for nanomaterials synthesis and surface Engineering, *Plasma Process.
494 Polym*, 9, 1074-1085

495 Nastase, R., Tatibouët, J-M., & Fourré, E. (2018) Depolymerization of inulin in the highly
496 reactive gas phase of a non-thermal plasma at atmospheric pressure. *Plasma Process and*
497 *Polymers*, 15, 1800067

498 National Research Council. *Plasma processing of materials: scientific opportunities and*
499 *technological challenges*. (1991) Washington, DC: The National Academies Press

500 Ong, HC., Chen, WH., Farooq, A., Gan, YY., Lee, KT., & Ashokkumar, V. (2019) Catalytic
501 thermochemical conversion of biomass for biofuel production: a comprehensive review,
502 *Renewable & Sustainable Energy Reviews*, 113, 109266

503 Pankaj, SK., & Keener, KM. (2017) Cold plasma: background, applications and current trends.
504 *Current Opinion in Food Science*, 16, 49–52

505 Postek, MT., Moon, RJ., Rudie, AW., & Bilodeau, MA. (2013) *Production and Applications*
506 *of Cellulose Nanomaterials*, Tappi Press

507 Raccuia, SA., Genovese, G., Leonardi, C., Bognanni, R., Platania, C., Calderaro P., & Melilli,
508 MC. (2016) Fructose production by *Cynara cardunculus* inulin hydrolysis, *Acta Horticulturae*,
509 43, 309-314

510 Ropartz, D., Bodet, P-E., Przybylski, C., Gonnet, F., Daniel, R., Fer, M., Helbert, W., Bertrand,
511 D., & Rogniaux, H. (2011) *Rapid Communication in Mass Spectrometry*, 25, 2059–2070

512 Shainsky, N., Dobrynin, D., Ercan, U., Joshi, SG., Ji, H., Brooks, A., Fridman, G., Cho, Y.,
513 Fridman, A., & Friedman, G. (2012) Plasma acid: water treated by dielectric barrier discharge,
514 *Plasma Process and Polymers*, 10, 1-6

515 Sheldon, RA. (2018) Chemicals from renewable biomass: a renaissance in carbohydrate
516 chemistry, *Current Opinion in Green and Sustainable Chemistry*, 14, 89-95

517 Shiomi, N., & Onodera, S. (1990) The ¹³C-NMR spectra of inulo-oligosaccharides,
518 *Agricultural Biological Chemistry.*, *54*, 215–216

519 Stevens, CV., Meriggi, A., & Booten, K. (2001) Chemical modification of inulin, a valuable
520 renewable resource, and its industrial applications, *Biomacromolecules*, *2*, 1-16

521 Sunka, P., Babicky, V., Lupek, MC., Lukes, P., Simek, M., Schmidt, J., & Cernak, M. (1999)
522 Generation of chemically active species by electrical discharge in water, *Plasma Sources*
523 *Science and Technology*, *8*, 258–265

524 Sylla-Iyarreta Veitía, S., & Ferroud, C. (2015) New activation methods used in green chemistry
525 for the synthesis of high added value molecules, *International Journal of Energy and*
526 *Environmental Engineering.*, *6*, 37-46

527 Takai, O. (2008) Solution plasma processing (SPP), *Pure and Applied Chemistry*, *80*, 2003-
528 2011

529 Tarabova, B., Lukes, P., Janda, M., Hensel, K., Sikurova, L., & Machala, Z. (2018) Specificity
530 of detection methods of nitrites and ozone in aqueous solutions activated by air plasma, *Plasma*
531 *Process and Polymers*, *15*, 1800030

532 Tendero, C., Tixier, C., Tristant, P., Desmaison, J., & Leprince, P. (2006) Atmospheric pressure
533 plasmas: a review, *Spectrochimica. Acta Part B*, *61*, 2-30

534 Wack, M., & Blaschek, W. (2006) Determination of the Structure and Degree of Polymerisation
535 of Fructans from Echinacea Purpurea Roots, *Carbohydrate Research*, *341*, 1147-53